EUROPEAN MECHANICAL SCIENCE
e-ISSN: 2587-1110

RESEARCH ARTICLE

Numerical simulation of a magnetic induction coil for heat treatment of an AISI 4340 gear

Önder Sönmez[1*], Deniz Kaya[1], Vladimir Bukanin[2], Aleksandr Ivanov[2]

[1]Akdeniz University, Faculty of Science, Department of Physics, Antalya, Turkey.
[2] Saint Petersburg Electrotechnical University, "LETI", St. Petersburg, Russian Federation.

Orcid: Ö. Sönmez (0000-0003-3356-5334), D. Kaya (0000-0002-1951-2466), V. Bukanin (0000-0002-0215-7621), A. Ivanov (0000-0002-9598-1344)

Abstract: In manufacturing industry, heat treatment is a fundamental requirement for improving the material quality of readily manufactured products. Induction heating technology is repeatable and easily controlled by the advantage of having an electronic control unit. Nowadays, numerical methods have gained so much importance that it becomes as a reference for the induction heating industry. Experimental methods are costly and time demanding procedures. However, making use of finite element method (FEA) software, induction heating simulations of a steel gear can be performed relatively cost effective and in a short time. In this paper, induction heating simulation of an AISI 4340 steel gear using FEA software is performed. The effect of variation of inductor frequency and air gap distance on the hardening depth of the gear surface is investigated. The temperature profile of the workpiece is obtained. From the temperature distribution on the steel gear workpiece, the regions of the gear at which the austenitizing temperature (Ac3) - responsible for martensite phase formation- are observed. From the numerical results, hardening profile and hardening depth of the gear is interpreted. During the induction and heating process, the temperature distribution on the AISI 4340 steel gear was determined, depending on the frequency change (medium frequency: 8 – 12 kHz) and the air gap variations (2 mm – 28 mm), using constant time (0.5 seconds), and constant coil power (220 kW). It is interpreted that as the coil frequency rise from 8 kHz to 12 kHz the temperature rises in the root region of the steel gear. This, consequently, leads to austenitizing temperature (800 °C) in deeper regions of the workpiece. On fixed time, constant power, and constant frequency (10 kHz), depending on the decrease in magnetic field effect, increasing the air gap from 2 - 28 mm led to reduced temperature in the root area (<800 °C).

Keywords: Induction heating; Numerical modelling; Hardness profile; Surface hardening; AISI 4340; Steel gear.

Nomenclature

AISI	American Iron and Steel Institute
FEA	Finite Element Analysis
4340	43 (1.8% Nickel, 0.8% Chrome, 0.25% Molybdenum) , 40 (0.4% Carbon)
ELTA	Electrothermal Analysis
CAD	Computer Aided Design
MF	Medium Frequency
HF	High Frequency
HV	Vickers Hardnes)
HRC	Rockwell Hardness on the C scale
Ac1	Lower Austenitizing Temperature
Ac3	Upper Critical Austenitizing Temperature

Greek letters

α	Temperature Resistance Constant
c_p	Specific Heat at Constant Pressure
f	Frequency
h	Heat Convection Coefficient
j	Current Density
k	Heat Conduction Coefficient
M	Modulus
μ_0	Magnetic Permeability İn Vacuum
μ_r	Magnetic Permeability İn Matter
n	Surface Normal Vector
q	Heat Flux
R	Radius
ρ	Density
ρ_0	Initial Resistivity
σ	Electrical Conductivity Coefficient
t	Time
T	Temperature
ω	Angular Frequency

1. Introduction

The technology of induction heating of gears emerged with the patent publication of W. Braun from the USA in 1926 and Vologdin V. P. from the Soviet Union in 1939 [1,2]. Nonetheless, the heat treatment dates too far more past, and it was long known and applied to improve

* Corresponding author.
Email: ondermetu@gmail.com

European Mechanical Science (2022), 6(2): 129-137
https://doi.org/10.26701/ems.1027181
Received: December 6, 2021 — Accepted: March 24, 2022

the mechanical properties of steel. High-carbon steel hardening has been used for thousands of years and this method is quite a basic procedure. Once the steel is heated sufficiently, and if it is immediately quenched into cold water, the steel workpiece turns into a reddish color. In this part, the steel apparently has a multicolored appearance and more importantly the mechanical properties are improved such as hardness. Although the heat treatment was in use since iron age, it was in the second quarter of 19th century whose mathematical methodology was fully comprehended. Yet, controlling the process electrically and full command on the consecutive physical phenomena was not well understood. But still, this heat treatment method was known for more than a hundred years [3]. This technology is commonly used for annealing, tempering, residual stress relieving and surface hardening of critical workpieces used in industry. The induction heating method for surface hardening has superiorities over alternatives due to its repeatability, eco-friendliness and being a practically rapid method [4,5].

Herein, numerical methods have gained as much importance as to become as a reference for the induction heating industry. Now due to numerical methods (finite element method, finite difference method), multiphysics simulation has been developed. This allows us to optimize the most important parameters of induction heating processes.

The induction heating multiphysics procedure involves the Faraday's law of induction, and resulting induction causes the eddy current which leads to the Joule effect phenomenon [6]. The result is the heating of the workpiece. These consecutive physical phenomena might seem simple; however, magnetic induction heating is quite a complicated phenomenon. For this reason, it is quite demanding procedure to design a magnetic induction heating system practically and usually it requires too many trials and error processes [7]. Besides, the experimental setup of magnetic induction system requires several equipment, e.g., temperature sensors, to place on various points through the workpiece. Apparently, these procedures and equipment take cost and time. In addition, the acquired data from sensors are not always reliable and precise regarding the experimental dynamics of the process. And with the same technique is required repeatedly for every single experiment.

Experimental methods are costly and time demanding due to the reasons mentioned above. However, using of finite element method software, induction heating simulations of a steel gear can be performed relatively cost effective and in a suitable time. While errors and mistakes during numerical experiment are costless, the numerical model can be optimized by sequential simulations and can be included into the manufacturing process [8]. Hence, the demand of numerical methods arises. In this multi-physical method, coupling of electromagnetic and thermal equations is complex and material properties are nonlinear. For this reason, many researchers put invaluable efforts to achieve a robust numerical solution for induction heating process [9]. There are simulation tools for induction heating system/component design which are readily being used in the academic studies [6,10,11]. An investigation on induction heating of AISI 4340 steel gear workpiece using simulation tool is carried out. In the induction heating system, the essentially focus was on the parameters such as hardening depth (mm) and power supply frequency (Hz). The numerical results and the plots of these results are obtained after performing consecutive simulations. In these plots, two valuable observable relations: expected hardening depth and coil excitement current-hardening depth are shown. Considerably fast numerical results owing to an additional numerical technique found in ELTA software are obtained [12].

2. Methods of Study

2.1. The Governing Equations

Transient heat conduction, Faraday induction law and Ohm law for joule heating is included in the model. In heat transfer modelling, to adopt more realistic approach, convection mode of heat transfer is included as well.

2-D transient heat transfer equation (Eq. 1), Faraday law of induction (Eq. 2) and Ohm's law (Eq. 3) are shown as following [13,14].

$$\rho c\frac{\partial T}{\partial t}+\nabla.\left(-k\nabla T\right)=q \tag{1}$$

$$j\omega\sigma A-\mu^{-1}\left(\nabla^2 A\right)=J_0 \tag{2}$$

$$\sigma=\frac{1}{\left|\rho_0\left(1+\alpha\left(T-T_0\right)\right)\right|} \tag{3}$$

where, ρ is mass density, c is specific heat capacity, T is temperature, k is thermal conductivity coefficient, q is auxiliary heat flux, j is current density, ω is angular frequency, σ is electrical conductivity coefficient, T_0 is ambient temperature, A is magnetic vector potential, μ is magnetic susceptibility of medium, ρ_0 is initial resistivity, J_0 is source current density applied for the coil and α is temperature coefficient of resistance.

Eq. (1) turns into Eq. (4) when convection and radiation modes of heat transfer is included into 2-D heat transfer equation [15].

$$k\frac{\partial T}{\partial n}+\alpha\left(T^4-T_0^4\right)+\beta\left(T-T_0\right)=0 \tag{4}$$

where, α is Boltzmann Constant and β is convection coefficient.

Skin effect is an active phenomenon when the current is alternating, and in this phenomenon the alternating current tends to flow nearer the outer surface of the conduc-

tor as the frequency of the alternative current increases. The skin (penetration) depth (δ) is expressed as in Eq. (5) [6].

$$\delta = \sqrt{2/(\omega\mu\sigma)} \tag{5}$$

Skin depth, denoted as δ, refers to 1/e of its value at the surface of the conductor. The current density in the conductor is expressed as in Eq. (6) [16],

$$j = j_0 * exp(-x/\delta) \tag{6}$$

Skin effect is a directly related phenomenon and can be mathematically expressed by the two equations Eq. (5,6). The current density in the material attenuates as the distance from surface increases. The skin depth is a function of frequency and material properties, as seen in Eq. (5). As the frequency increases, the depth of current density decreases. In Eq. (6), one can have an insight into how the current density near the surface of the material behaves as a function of radial distance. These two equations are direct outcomes of AC current.

2.2. The Material Properties and Simulation Setup

The material characteristics determine the skin (penetration) depth. The magnetic permeability (μ) and the electrical conductivity or specific resistance (ρ) of the material are temperature dependent. Using this property, controlling the skin (penetration) depth becomes practicable. AISI 4340 steel is a type of ferromagnetic material with a higher relative magnetic permeability, which enables a smaller skin effect. The composition of the ferromagnetic material highly affects the property of magnetic permeability (μ). The other factor that determines the magnetic permeability is the Curie temperature, above which the material loses its magnetization [15]. Due to the loss of magnetization, the skin depth suddenly increases in this condition (760 ^{0}C). The Curie temperature is critical through the induction heating process for this reason.

The AISI 4340 material is a low alloy steel containing nickel chromium and molybdenum elements. AISI 4340 steel is highly suitable for induction heating due to its alloy element and carbon content that contribute to hardening. AISI 4340 steel is a commonly known material in terms of toughness, high hardness after heat treatment, as well as fatigue resistance properties. Typical field of use of AISI 4340 steel is mainly, aerospace industry: landing gears of airplanes, gear wheels, shafts, and other structural elements for power transmission [15,17-19]. A proper identification of material properties is extremely important for a robust numerical simulation. For this reason, transformation temperatures and critical temperatures should be known for AISI 4340 steel material. In Table 1, the material properties of the AISI 4340 steel material are shown below.

Table 1. Material properties for AISI 4340 steel

Heat Rate [°C/s]	Ac1 [°C]	Ac3 [°C]	Acm [°C]
2739	726	983	1058
814	787	982	1048
427	778	949	1038
99	768	856	910

The AISI 4340 steel is a high strength material mostly preferred as gear material due to its superior mechanical properties. In the content of this alloy, the presence of chromium, nickel, and molybdenum enables the alloy to be suitable for induction heating process for surface hardening [3]. AISI 4340 is also commonly known for its toughness, high strength, and fatigue resistance. The heat treatment of AISI 4340 has therefore of great importance. The chemical composition of AISI 4340 steel is given in Table 2. by element and the percentage.

Table 2. Chemical composition of AISI 4340 steel

Element	Fe	Ni	Cr	Mn	C	Mb	Si	Cu
Percentage (wt. %)	95.99	1.61	0.88	0.6	0.42	0.29	0.18	0.03

The simulation procedure is illustrated as a flow chart which is given in Figure 1.

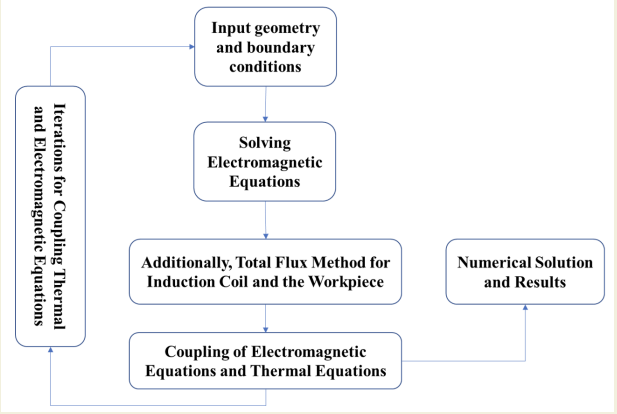

Figure 1. The flow chart of the overall simulation procedure.

In algorithm of ELTA 7.0 Software, finite difference method is used to obtain the solution of coupled electromagnetic and thermal equations. Additionally, in the numerical solution process, an analytical method "Total Flux Method" is introduced to account for the coil and workpiece. This additional analytical method is proposed by V. Nemkov [1].

In ELTA software, half part of the single tooth is taken as workpiece geometry due to symmetry (Figure 2).

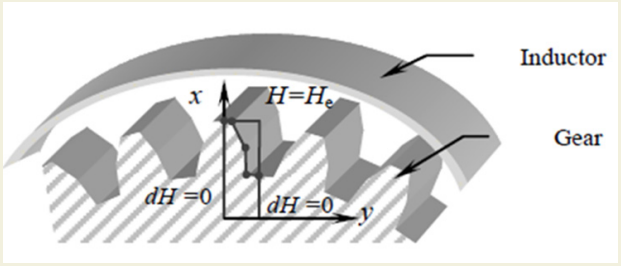

Figure 2. 2-D geometry model for calculation in ELTA software [20]

The internal part of electro-thermal problems is solved by considering geometrical symmetry, i.e., only 1/2 part of one gear tooth is calculated. ELTA 7.0 calculates in this part of workpiece the two-dimensional distribution of power sources and temperature.

The non-linear differential equation for magnetic field H and temperature T are described as:

$$\frac{\partial}{\partial x}\left(\rho \frac{\partial \dot{H}}{\partial x}\right) + \frac{\partial}{\partial y}\left(\rho \frac{\partial \dot{H}}{\partial y}\right) = j\omega\mu\mu_0 \dot{H} \quad (7)$$

$$C_v \frac{\partial T}{\partial t} = \frac{\partial}{\partial x}\left(\lambda \frac{\partial T}{\partial x}\right) + \frac{\partial}{\partial y}\left(\lambda \frac{\partial T}{\partial y}\right) + w, \quad (8)$$

where ρ – electrical resistivity, ω – angular frequency, μ – permeability, x, y – coordinates of workpiece cross-section, C_v – volume specific heat, λ – thermal conductivity, w – heat source density, T – temperature, t – time. The boundary conditions are known magnetic strength H_e on the surface in the air gap between inductor and gear, symmetry in central parts of face and bottom ($dH = 0$), super-magnetic ($H = 0$) or normal component of current is equal to 0 in the main body of a gear wheel (line $x = 0$) and temperature-dependent heat losses on the gear surface during the forced cooling stage, included in the program database.

As illustrated in Figure 2, the path of the profile of the gear tooth is represented by 5 points with 4 straight lines. For gear parameters the setting window is shown in Figure 3.

The gear parameters in this study: AISI 4340 steel is the material of the gear, outside diameter is (Do) 10.52 cm, root diameter (Dr) is 8.67 cm, the interior diameter (Dint) is 1 cm, face width (Zg) is 0.65 cm and pitch diameter (Dp) are 9.595 cm. The number of teeth of the gear (N) is 48. The processing parameters are shown in the Figure 4 below. The processing parameters are: 220 kW power of power source and a range of frequency 8-10-12 kHz.

As given in Figure 5, the interior radius of the inductor (R1) is 5.71 cm (11.42 cm diameter) with a turn number 1. The profile of the inductor is selected as 6.5 x 30 x 3 mm. The simulation time setting is 0.5 seconds. The geometry of the inductor is a hollow rectangle with a gap in the middle of its cross section for water cooling. Re indicates exterior radius of the workpiece.

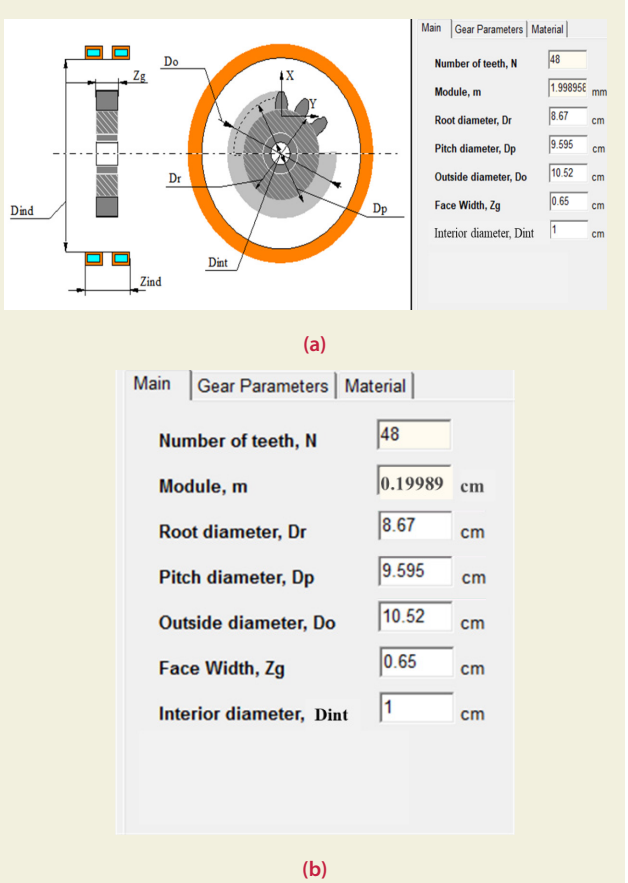

Figure 3. (a) Gear geometry and dimensions (b) Input parameters window

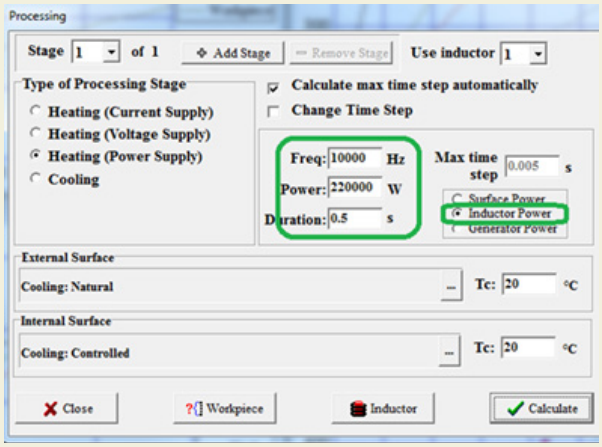

Figure 4. Gear processing settings in ELTA

The temperature distribution in the AISI 4340 steel gear workpiece was analyzed using ELTA software, using inputs of 220 kW of power, 10 kHz coil frequency, 4.54 mm clearance distance and 0.5 seconds simulation time. The temperature behavior is obtained for three different frequencies (8, 10 and 12 kHz).

There are numerous numbers of research findings that propose medium frequency (MF) of alternating current

frequency range is preferably used in practice [9,17,21-24]. As a result of simulation outcomes which made grounds for this paperwork, a couple of kHz of frequency (MF) for alternating current range, a couple of kW power, a few millimeters of airgap distance have offered a desirable depth of penetration of temperature which is required for a considerable depth of hardness. In this study, these simulation parameters and geometry dimensions are replicated by modelling the same case taken from one of an academic paper of Noureddine Barka [25]. This mentioned study is used for validation purpose which can be seen on Fig 11. After validating the current model using ELTA software and being ensured of the results referencing the study of Barka, N. [25] , a close range of these simulation parameters are swept parametrically in order to observe the effect of variation of inductor frequency and the air gap distance on the hardening depth of the gear surface.

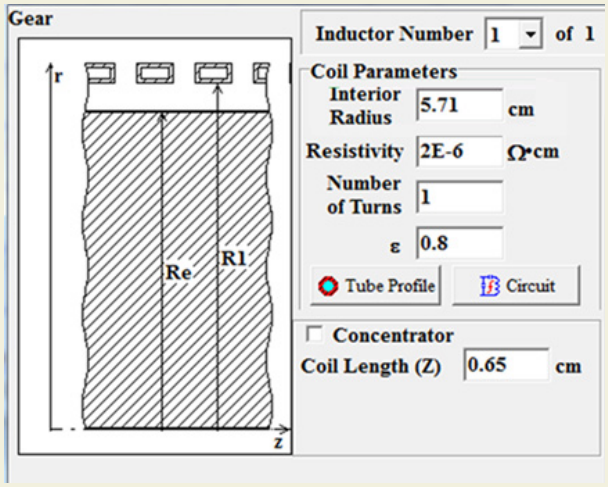

Figure 5. Inductor parameters

3. Results and Discussion

The parameter arrangements are determined by holding heating time and coil power fixed, and the coil frequency and air gap value. Under this arrangement the hardening depth for each case is obtained. The main goal was to achieve a minimum temperature over 800 ^{0}C (austenitizing temperature, Acm) and observe a uniform temperature distribution. For the parameter arrangements: heating time = 0.5 s, coil power 220 kW, coil frequency (8,10,12 kHz) and air gap value (2, 4.54, 7, 9, 11, 16, 20, 24, 28 mm) a set of cases between the combinations were performed among these parameters. The air gap of 4.54 mm value is the reference value from Barka, N. [25].

In case of 8 kHz coil frequency, the temperature in the root area of the 4340 steel gear workpiece reaches to 800 °C at a depth of 0.35 mm (Figure 6.a, cyan line limit). In the case where the coil frequency is 10 kHz, it is observed that the critical austenitizing temperature (800 °C) for martensite formation occurs at a depth of 1.48 mm, and if the frequency is increased to 12 kHz, this temperature is observed at a depth of 2.75 mm (See Figure 6.b and Figure 6.c, cyan line boundary). Therefore, as the frequency increased from 8 kHz to 12 kHz at three different frequencies, the martensite phase formation is observed at deeper regions. This formation of martensite phase is critical for fatigue and wear resistance for the workpiece. The change of the depth in which the austenitizing temperature occurs at a constant distance (4.54 mm) is shown in Figure 7.

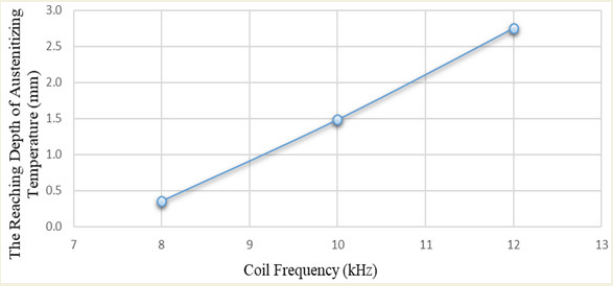

Figure 7. Change of the reaching depth of austenitizing temperature depending on the coil frequency

In the study, the effect of the air gap and the induction coil on the temperature distribution and hardness depth were examined. Therefore, the coil power (220 kW) coil frequency (10 kHz), heating time (0.5 seconds) were kept constant, and the air gap was changed (2, 4.54, 7, 9, 11, 16, 20, 24, 28 mm). The results were plotted, it is seen in figure 8 and three of these cases are shown as temperature in Figure 8.

In the case in which the air gap is 4.54 mm, a temperature of 800 ^{0}C was reached at a depth of 1.48 mm at the root region (Figure 8a). Since the magnetic field effect decreases due to the increase in the distance between the workpiece and the coil, the temperature increase on the workpiece is limited. Therefore, in cases where the air gap is 16 mm and 28 mm, the austenitizing temperature (800 ^{0}C) - required for martensite formation - occurs at a limited depth in the root region of the workpiece (Figure 8b and Figure 8c). In Figure 9, the formation depth of the austenitizing temperature versus air gap is given. As shown in Figure 9, increasing of the air gap leads to a decrease in the depth of martensite formation in the induction heating process. It is important in terms of wear resistance and fatigue resistance.

Consequently, a prescription of desired induction heating system parameters is carried out. The dimensions, appropriate power and the frequency parameters of the inductor, the air gap are well-defined as a result of this study. Applying the determined system parameters, the induction heating for the selected gear gives even temperature distribution and adequate depth of hardening. Furthermore, preparing all the simulation setup and obtaining the results were too simple by the help of rapid running ELTA software.

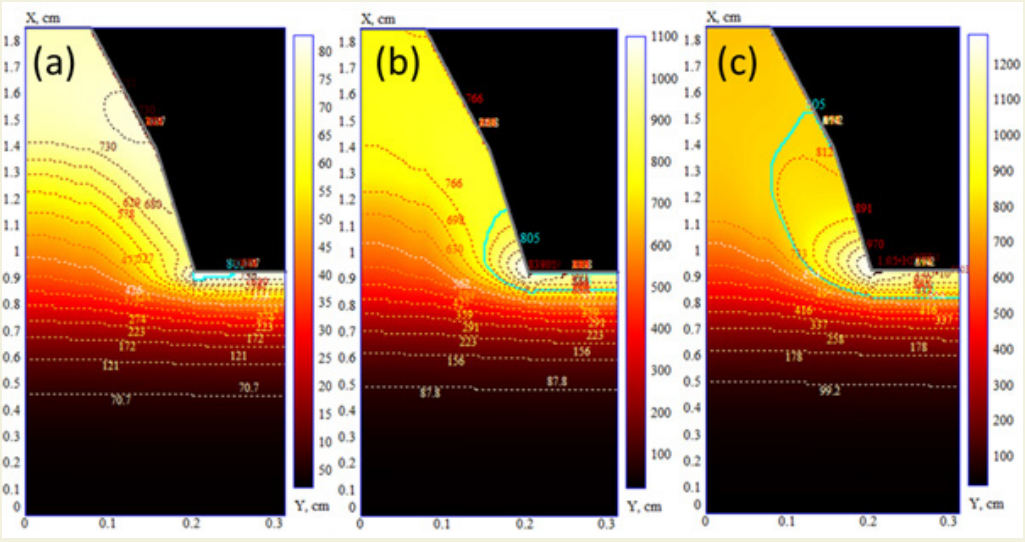

Figure 6. Fixed air gap (4.54 mm), heating time (0.5 seconds) and coil power (220 kW). The temperature distribution when coil frequency is (a) 8 kHz (b) 10 kHz (c) 12 kHz.

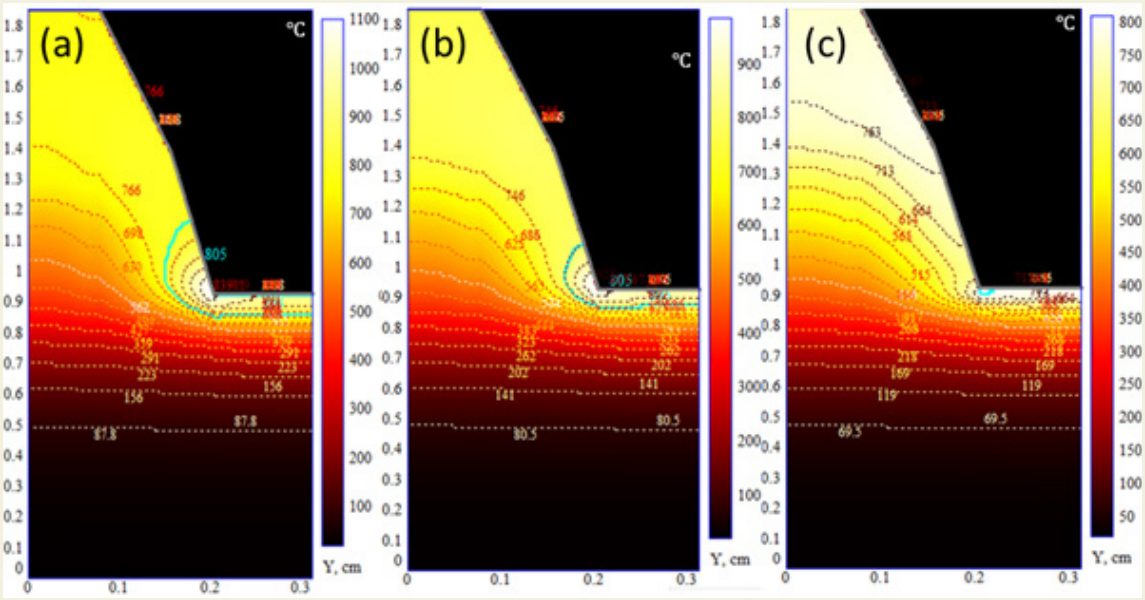

Figure 8. The effect of three different values of the air gap using coil frequency (10 kHz), coil power (220 kW), heating time (0.5 seconds) on temperature distribution (a) 4.54 mm (b) 16 mm (c) 24 mm.

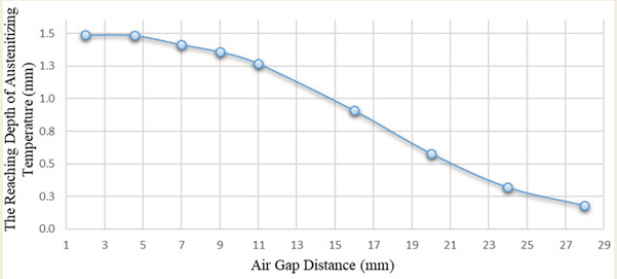

Figure 9. At fixed heating time, coil power and coil frequency, the variation of the temperature of the austenitizing temperature (800 °C) by the air gap.

In this study, the induction heating process for the AISI 4340 steel gear workpiece was studied using ELTA software. During the induction and heating process, the temperature distribution on the AISI 4340 steel gear was determined, depending on the frequency change (medium frequency: 8 – 12 kHz) and the air gap variations (2 mm – 28 mm), using constant time (0.5 seconds), and constant coil power (220 kW). In the case of constant time, constant power, and constant air gap (4.54 mm), the increase of the frequency from 8 kHz to 12 kHz has led to increased temperature in the root region of the steel gear. This, consequently, end up with the austenitizing temperature (800 ^{0}C) in deeper regions of the workpiece. On fixed time, constant power, and constant frequency (10 kHz), depending on the decrease in magnetic field effect, increasing the air gap from 2 mm to 28 mm led to reduced temperature in the root area (<800 ^{0}C).

In induction heating, it is very important to achieve an induced temperature at a certain depth. Thus, workpiece

wear resistance and fatigue resistance can be improved by using further heat treatment. To achieve this goal, induction heat treatment parameters were determined for a specific gear geometry using ELTA software. When the induction coil geometry has a section area of 6.5 x 30 mm, the coil frequency is 10 kHz, and the 4-5 mm of distance between the workpiece and coil the simulation outcome is formation of martensite at a depth of 1.48 mm in the root area of gear workpiece. In induction heating common process, medium frequency (MF) which is a generally a couple of kHz, is used in this study. As one of the outcomes of the study, it is observed that when the coil frequency was 8 kHz, the hardening depth of the gear in the root area was 0.35 mm, and when the coil frequency was 12 kHz the depth of hardening in the root area was 2.75 mm.

The outcomes obtained from this study can be compared with references and experimental studies for validation purpose. In this study, the induction heating process for AISI 4340 steel gear workpiece was investigated using ELTA software and the temperature distribution and hardness formation were compared with the work of Barka et al. [25] with COMSOL software.

The temperature distribution obtained by Barka et al. [25] using COMSOL software is given in Figure 10. When the temperatures in the tooth tip and tooth root regions were compared, it was observed that the current work and the work of Barka et al [25] have a good agreement (Figure 10). In addition, in Figure 10, the austenitization temperature (Ac3 temperature) is shown at a depth of 1.48 mm (turquoise line) with the ELTA software. This means that in the cooling process after the induction heating process, the martensite phase, which provides hardness increase and fatigue resistance, can be formed up to a depth of 1.48 mm in the root region of the gear.

The temperature distributions obtained for the 4340 steel gear workpiece with the use of ELTA and COMSOL software help us understand in which regions the martensite phase occurs after the cooling process and thus to determine the hardness profile. The austenitization temperature (Ac3, 800°C) of the AISI 4340 steel material was used to obtain the hardness profile. In the temperature distribution obtained using ELTA software in Figure 11, the region within the turquoise border shows the region where the temperature is 800°C and above. After this temperature distribution is achieved, martensite phase formation will occur in this region in 4340 steel workpieces with the quenching process. In the temperature distribution obtained by using COMSOL software in Figure 11, the gray region shows the region where the temperature is 800°C and above. Similarly, in the cooling process from this region, the entire gray region will turn into martensite phase. Therefore, by choosing the appropriate induction and coil parameters, determining the temperature profile for a steel gear workpiece, and determining the regions where the martensite phase occurs accordingly will help us obtain the desired results in terms of wear and fatigue resistance.

The air gap is another practically important variable. In the study, as the air gap is increased, the temperature in the gear root area decreased and it is interpreted that it did not cause the desired hardness change. In this study, ELTA 7.0 is used for the analysis of induction heating process of an AISI 4340-steel gear workpiece. Using ELTA software, one could rapidly perform induction heating simulation. Gears made of AISI 4340 steel are critical

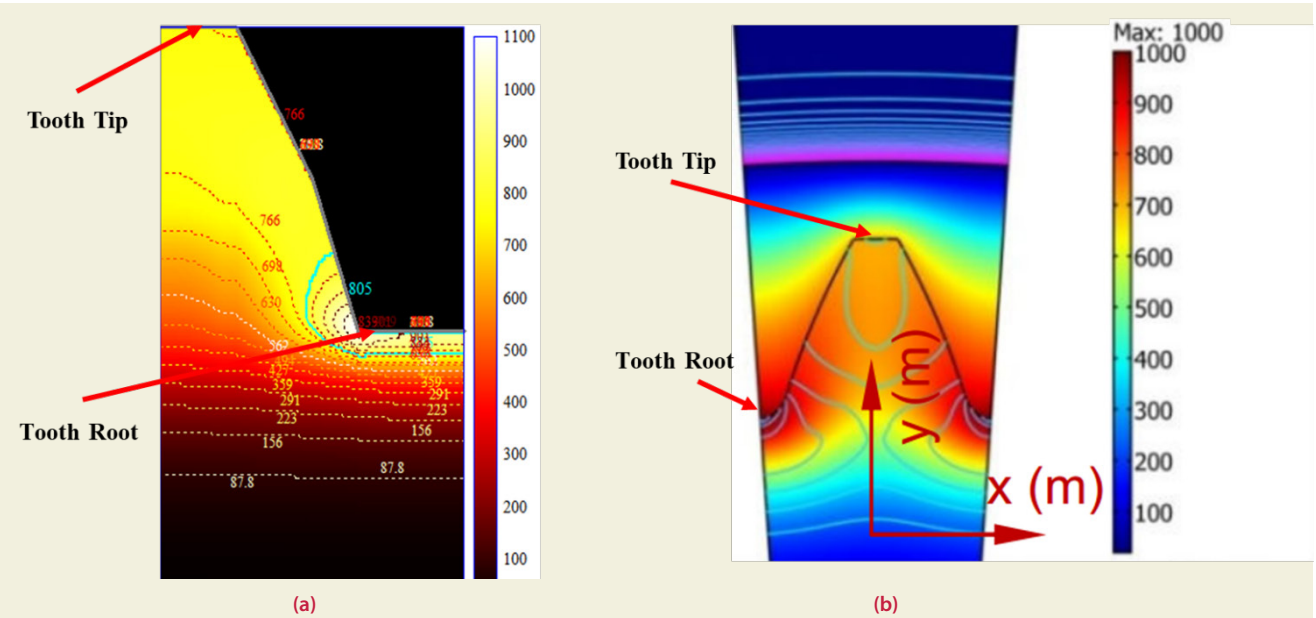

(a) (b)

Figure 10. Temperature distributions obtained on 4340 steel gear workpieces using ELTA software and COMSOL software (coil power 220 kW, toot tip region to coil distance 4.54 mm, coil frequency 10 kHz and induction heating time 0.5 seconds) (a) ELTA 7.0© (b) COMSOL-reference study [25]

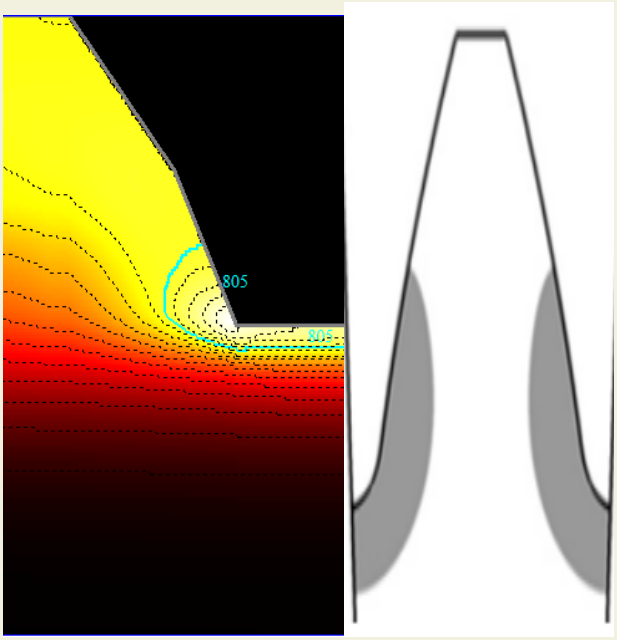

Figure 11. Hardness profile extracted from temperature distributions obtained on 4340 steel gear workpieces using ELTA software and the reference study with COMSOL software (coil power 220 kW, toot tip region to coil distance 4.54 mm, coil frequency 10 kHz and induction heating time 0.5 seconds) (a) ELTA 7.0© (zone within turquoise border) (b) COMSOL-reference study (grey zone) [25]

parts for aerospace industry. For this reason, enhancement of mechanical properties of this workpiece from workpiece is particularly important for the related industries. Since these critical components are operating under high torque and force loads along with contact with other moving parts, the fatigue, toughness, and hardness properties are the key features to be improved for operational performance of these critical components. The lifetime of these parts is strongly dependent to the heat treatment processes they undergo before the launch of the product. Consequently, the heat treatment processes must be proper and precise to be able to improve the mechanical properties of these critical components. Using numerical methods in this study, we make sure that the key parameters for induction hardening process are precisely determined for a better outcome. In the future studies related to this field, high frequency effect (100-200 kHz), coil geometry effect, and the effect of cooling water can be studied. In addition, the application of two consecutive frequencies (medium-frequency and high frequency) can be examined with magnetic flux concentrator.

Acknowledgments

The authors would like to thank to V. Bukanin and A.N. Ivanov for valuable discussions, remarks, and academic trial version of ELTA software from NSGSOFT.

Declaration of Competing Interest

The authors declare that they have no known competing financial interests or personal relationships that could have appeared to influence the work reported in this paper.

Rererences

[1] Bukanin, V. A., Ivanov, A. N., Zenkov, A. E., Vologdin, V. V., & Vologdin Jr, V. V. 2018. Induction Hardening of External Gear. Management Science and Engineering, 327(2), 022016. https://doi.org/10.1088/1757-899X/327/2/022016

[2] Dawson, F. P., & Jain, P. 1990. Systems for induction heating and melting applications: a comparison of load commutated inverter. In 21st Annual IEEE Conference on Power Electronics Specialists (pp. 281-290). IEEE.

[3] Magnabosco, I., Ferro, P., Tiziani, A., & Bonollo, F. 2006. Induction heat treatment of an ISO C45 steel bar: Experimental and numerical analysis. Computational materials science, 35(2), 98-106. https://doi.org/10.1016/j.commatsci.2005.03.010

[4] Jomaa, W., Songmene, V., & Bocher, P. 2013. On residual stress changes after orthogonal machining of induction hardened AISI 4340 steel. In Proceedings of Materials Science and Technology Conference and Exhibition, MS&T, 13, 94-103.

[5] Lucia, O., Acero, J., Carretero, C., & Burdio, J. M. 2013. Induction heating appliances: Toward more flexible cooking surfaces. IEEE Industrial Electronics Magazine, 7(3), 35-47.

[6] Jankowski, T. A., Pawley, N. H., Gonzales, L. M., Ross, C. A., & Jurney, J. D. 2016. Approximate analytical solution for induction heating of solid cylinders. Applied Mathematical Modelling, 40(4), 2770-2782. https://doi.org/10.1016/j.apm.2015.10.006

[7] Tavakoli, M. H., Ojaghi, A., Mohammadi-Manesh, E., & Mansour, M. 2009. Influence of coil geometry on the induction heating process in crystal growth systems. Journal of crystal growth, 311(6), 1594-1599. https://doi.org/10.1016/j.jcrysgro.2009.01.092

[8] Chaboudez, C., Clain, S., Glardon, R., Rappaz, J., Swierkosz, M., & Touzani, R. 1994. Numerical modelling of induction heating of long workpieces. IEEE transactions on magnetics, 30(6), 5028-5037.

[9] Fu, X., Wang, B., Tang, X., Ji, H., & Zhu, X. 2017. Study on induction heating of workpiece before gear rolling process with different coil structures. Applied Thermal Engineering, 114, 1-9. https://doi.org/10.1016/j.applthermaleng.2016.11.192

[10] Baldan, M., Cetin, M., Nikanorov, A., & Nacke, B. 2019. Optimal Design of Magnetic Flux Concentrators in Induction Heating. In 2019 XXI International Conference Complex Systems: Control and Modeling Problems (CSCMP) (pp. 203-207). IEEE.

[11] Bukanin, V., Ivanov, A., & Zenkov, A. 2019. Investigation of heating and melting in ELTA programs. COMPEL-The international journal for computation and mathematics in electrical and electronic engineering.

[12] Bukanin, V. A., Zenkov, A. E., & Ivanov, A. N. 2017. Simulation of single and dual-frequency induction hardening of steel gear using ELTA. In 2017 IEEE Conference of Russian Young Researchers in Electrical and Electronic Engineering (EIConRus) (pp. 791-795). IEEE.

[13] M. Fisk. 2011. Simulation of induction heating in manufacturing. International Journal for Computational Methods in Engineering Science and Mechanics,12,161-167.

[14] Chen, H. C., & Huang, K. H. 2008. Finite element analysis of coupled electromagnetic and thermal fields within a practical induction heating cooker. International Journal of Applied Electromagnetics and Mechanics, 28(4), 413-427.

[15] Candeo, A., Ducassy, C., Bocher, P., & Dughiero, F. (2011). Multiphysics modeling of induction hardening of ring gears for the aerospace industry. IEEE Transactions on Magnetics, 47(5), 918-921.

[16] Frogner, K., Andersson, M., Cedell, T., Siesing, L., Jeppsson, P., & Ståhl, J. 2011. Industrial heating using energy efficient induction technology. In Proc. Int. Conf. Manuf. Syst. (pp. 1-6).

[17] Hadhri, M., El Ouafi, A., & Barka, N. 2017. Prediction of the hardness profile of an AISI 4340 steel cylinder heat-treated by laser-3D and artificial neural networks modelling and experimental validation. Journal of Mechanical Science and Technology, 31(2), 615-623.

[18] Pape, J. A., & Neu, R. W. 2007. A comparative study of the fretting fatigue behavior of 4340 steel and PH 13-8 Mo stainless steel. International journal of fatigue, 29(12), 2219-2229.

[19] Maamri, I., El Ouafi, A., & [2], N. 2014. Prediction of 4340 steel hardness profile heat-treated by laser using artificial neural networks and multi regression approaches. International Journal of Engineering and Innovative Technology, 4(6), 14-22.

[20] Bilal, M. M., Yaqoob, K., Zahid, M. H., Tanveer, W. H., Wadood, A., & Ahmed, B. 2019. Effect of austempering conditions on the microstructure and mechanical properties of AISI 4340 and AISI 4140 steels. Journal of Materials Research and Technology, 8(6), 5194-5200.

[21] Barka, N., Bocher, P., Chebak, A., Brousseau, J., & Ramdenee, D. S. (2011). Study of Currents and Temperature of Induced Spur Gear using 2d Simulation. International Journal of Mechanical and Mechatronics Engineering, 5(11), 2483-2488.

[22] Di Barba, P., Forzan, M., & Sieni, E. (2015). Multiobjective design optimization of an induction heating device: A benchmark problem. International Journal of Applied Electromagnetics and Mechanics, 47(4), 1003-1013.

[23] Smalcerz, A. (2015). The use of multifrequency induction heating for temperature distribution control. Archives of metallurgy and materials, 60.

[24] Chebak A., Barka N., Menou A., Brousseau J.and Ramdenee D., (2011). Simulation and validation of spur gear heated by induction using 3D multi-physics model. World Academy of Science, Engineering and Technology,Vol. 59, 893-897.

[25] Barka, N., (2017). Study of the machine parameters effects on the case depths of 4340 spur gear heated by induction—2D model. The International Journal of Advanced Manufacturing Technology, 93(1-4), 1173-1181.